# Stress measurements for underground powerhouses – three recent cases

**L. Lamas[1], M. Espada[1], B. Figueiredo[2], and J. Muralha[1]**

[1]National Laboratory for Civil Engineering – LNEC, Lisbon, Portugal
[2]Formerly at LNEC, currently at Uppsala University, Sweden

Release of the *in situ* state of stress is often the most relevant action during the excavation of underground structures in rock masses, such as powerhouse caverns for hydroelectric schemes, which are often excavated at great depth and have large dimensions. Design of the supports, namely using numerical models, requires an estimate of the magnitude and direction of the principal stresses. However, a large number of factors influence the *in situ* stress field and its characterisation is a difficult task. Besides, the number of tests carried out for determination of the *in situ* stresses in rock masses is usually small, due to cost and time constraints, and all the testing methods have limitations inherent to their nature.

The paper presents methodologies for analysis of the stress field obtained from the results of *in situ* stress measurements using three methods: overcoring, hydraulic fracturing and flat jacks. These methodologies integrate all stress measurements and use numerical models of the rock mass that represent the ground topography, the lithology, and the geometry of the underground openings, so that the most likely stress field in the zone of interest for the design is obtained. Instances of application to three underground powerhouses are presented.

## INTRODUCTION

Powerhouse caverns are underground structures of relevance in the design of hydroelectric projects. In power schemes with high water head in mountainous regions, the power conduit is often built underground. Thesual reasons for this are the better quality of the rock mass at depth and the higher *in situ* stresses, which enable the construction of unlined pressure tunnels and shafts, with economic advantages. The increase in the number of reversible, pump-storage projects, where the hydraulic power units (pump turbines) must be located considerably below the downstream water level, also calls for the construction of large underground powerhouses at great depth, which often exceeds 500 m.

In power conduits with long, high pressure, headrace tunnels, characterisation of the *in situ* state of stress is important for establishing the alignment of the conduit, in order to avoid the occurrence of hydraulic jacking and uncontrolled leakage. Owing to the length of these tunnels, usually a limited number of *in situ* stress measurements is carried out, and empirical rules are used to locate the power conduit deep enough, so that the internal water pressure never exceeds the minimum *in situ* stress.

Underground powerhouses pose specific problems, because they are not linear constructions like tunnels, with great length and constant cross section. They are spatially more concentrated, but often have complex geometries and large dimensions. Typical spans of powerhouse caverns range from 15 m to 25 m and depend on the size of the power units. The height is greater at the location of the power units, where it can reach values close to 100 m, whereas the length depends on the number of power units and often exceeds 100 m. Water inlets and outlets connect to the cavern, as well as several galleries and shafts for access and services. Powerhouse caverns are located close to other large openings, such as surge tanks and chambers for transformers and valves, adding to the geometric complexity of these underground structures.

In terms of geotechnical conditions, designers try to locate these large openings in zones of good quality rock mass, without major faults and variations of geology. Selection of such locations is based on the results of adequate site investigation programmes, including stress measurements and deep boring to the proposed location. Ideally, when high horizontal *in situ* stresses are present, the longitudinal axis of the caverns should be aligned with the maximum horizontal stress. However, it should be borne in mind that there are other criteria that influence the cavern location and orientation, namely those related with the hydraulic behaviour of the power conduit or the mechanical behaviour of the equipment, which sometimes impose stronger constraints and often prevail. Therefore, the final location and orientation of a powerhouse cavern is not always optimised from the geotechnical point of view.

Construction of deep powerhouse caverns, with complex geometry, large dimensions and high *in situ* stresses, requires the planning of the different excavation phases, which must consider the optimisation of the time schedule and excavation costs, as well as the stability of the openings during the entire excavation sequence.

The support systems for these complex structures are nearly always flexible, allowing the deformation of the rock mass to contribute to the overall strength and thus to the stability of the openings. In most cases the support is composed of fibre reinforced sprayed concrete with typical thickness of a few tens of centimetres and systematic rock bolts with lengths that can exceed 10 m. These support systems must be designed taking into consideration the potential failure mechanisms, namely controlled by the rock mass structure, by the brittle behaviour of highly stressed good quality rock, or by the deformational behaviour and plastic zones of the rock mass (see, for instance, Laigle and Plassart, 2015).

The design of powerhouse caverns, including the definition of the excavation sequence and of the support system, requires the use of numerical models. The numerical analyses may be used to simulate plausible failure mechanisms and ensure adequate safety against them (ultimate conditions), or to simulate the expected behaviour during excavation and operation, namely the expected deformational behaviour (serviceability conditions). Depending on the objectives of the models and on the plausible failure mechanisms, continuous or discontinuous analyses can be justified, and linear elastic or nonlinear rock mass behaviours considered.

The main actions to consider in the numerical modelling of the excavation are the self-weight of the rock mass and the release of the *in situ* stresses. The self-weight is mainly important for the stability of isolated rock blocks or rock blocks assemblies in structurally controlled failure modes, as well as for continuous analyses at shallow depths. The release of the *in situ* stresses has to be considered for the various failure modes, but also for the numerical analyses of serviceability conditions. The calculated displacements are essential information for monitoring the behaviour of the underground structure during the excavation process, thus allowing to ensure safety during construction.

An adequate estimate of the initial stress field in the rock mass at the powerhouse location is needed. However, the large number of factors that influence the *in situ* stress field makes its characterisation a difficult task. These factors include lithological or deformability heterogeneities, discontinuities, topography, the existence of nearby excavations, tectonic forces, and time dependent effects at the geological scale. Besides, tests for determination of the *in situ* stresses in rock masses are usually few in

number due to cost and time constraints, they have limitations inherent to their nature, and their results are valid only in the locations where they are executed.

Owing to these factors, characterisation of the *in situ* stress field in the rock mass at the powerhouse location requires execution of *in situ* tests using the most appropriate test techniques and a global interpretation model for analysis of their results. The stress field estimated in such way can be used as input to the numerical models for calculation and design purposes.

Several stress measurement programmes have been undertaken in the last decade for design of large powerhouse caverns in the north of Portugal. This paper summarises the testing methods that were used and some relevant features of the testing programmes. The methodologies for analysis of the stress field obtained from the results of *in situ* stress measurements using the overcoring, hydraulic fracturing and flat jack methods are presented. These inverse methodologies use numerical models of the rock mass that represent the ground topography, the lithology and the underground openings, so that, given the results of all the stress measurements, the most likely stress field in the zone of interest for the design of the underground structures is obtained. Instances of application to the underground powerhouses of Paradela II and Salamonde II (owned by EDP – Energies of Portugal, S.A.), and of Gouvães (owned by Iberdrola, S.A.) are presented. Finally, the results of an investigation of the influence of time dependent effects on the stress field are briefly presented.

## TESTING METHODS

### General

Several authors present descriptions, limitations and fields of application of existing *in situ* stress measurement methods (e.g. Cornet 1993; Amadei and Stephansson, 1997; Fairhurst, 2003; Hudson *et al.*, 2003; Ljunggren *et al.*, 2003). They are usually grouped into methods based on hydraulic fracturing; methods based on the complete stress release; methods based on the partial stress release; and methods based on the observation of the rock mass behaviour. In the cases presented in this paper overcoring, flat jack and hydraulic fracturing tests were performed.

Overcoring and hydraulic fracturing tests are used when the zones of interest can only be reached with boreholes, in most cases during the geotechnical survey stage. Flat jack tests require direct access to rock mass surfaces, so they are usually performed when excavation reaches the zones near to the caverns. Often their results are used to confirm previous stress field estimates. Hydraulic fracturing tests reported in this paper were performed in collaboration with the University of Strasbourg.

### Overcoring

Overcoring tests use a complete stress release method allowing all six stress tensor components at a given location in a borehole to be determined. In these studies, LNEC's STT (strain tensor tube) triaxial cells were employed. They are 2 mm thick epoxy resin hollow cylinders with 10 embedded strain gauges. The test starts by cementing the cell inside a 37 mm diameter borehole. Then the *in situ* stresses are released by overcoring with a larger diameter bit. Strains are measured during overcoring and until temperature stabilises by an in-built data-logger, and the stresses are calculated using the rock elastic constants obtained in a biaxial test on the recovered core with the cemented cell. Figure 1 illustrates an STT cell with the data logger, a biaxial test chamber and a diagram with the typical evolution of the measured strains and temperature during the overcoring process.

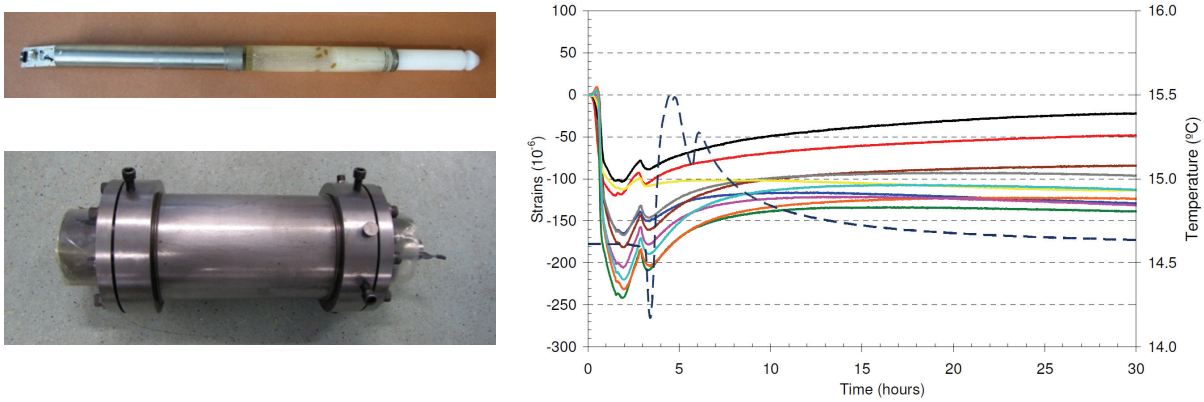


*Figure 1. Overcoring gauge, biaxial test chamber, and typical strains measured during overcoring.*

**Flat Jacks**

The flat jack method is based on partial stress release. LNEC's SFJ (small flat jack) test consists of cutting a 10 mm slot in a rock surface, with a 600 mm diameter circular disk saw, where a flat jack is inserted. Pressure is applied by the flat jack until the deformation caused by opening of the slot is restored. With each flat jack, a single stress component is obtained. Usually, at a given location, several tests in slots with different orientations are performed (Figure 2).

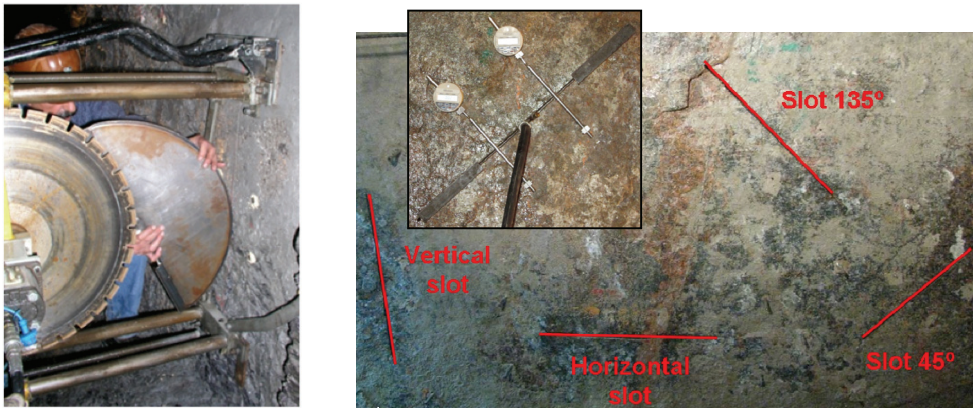


*Figure 2. Flat jack being inserted in the slot, array of slots and instrumentation.*

**Hydraulic Fracturing**

Two types of hydraulic tests—hydraulic fracturing (HF) and hydraulic tests on pre-existing fractures (HPTF)—were performed by the University of Strasbourg, together with LNEC's overcoring and flat jack tests, in a study for the design of a 500 m deep cavern (Figueiredo, 2013). HF tests induce a fracture in the rock by applying water pressure in a borehole section isolated by packers, enabling the minimum horizontal stress to be estimated. In HTPF tests, water pressure is applied in a borehole intersecting an isolated existing fracture, the opening of which allows the stress component perpendicular to the fracture plane to be determined. Figure 3 shows the hydraulic fracturing equipment being inserted in a borehole, an electrical image of a tested fracture and a scheme with the general setup for the hydraulic fracturing tests.

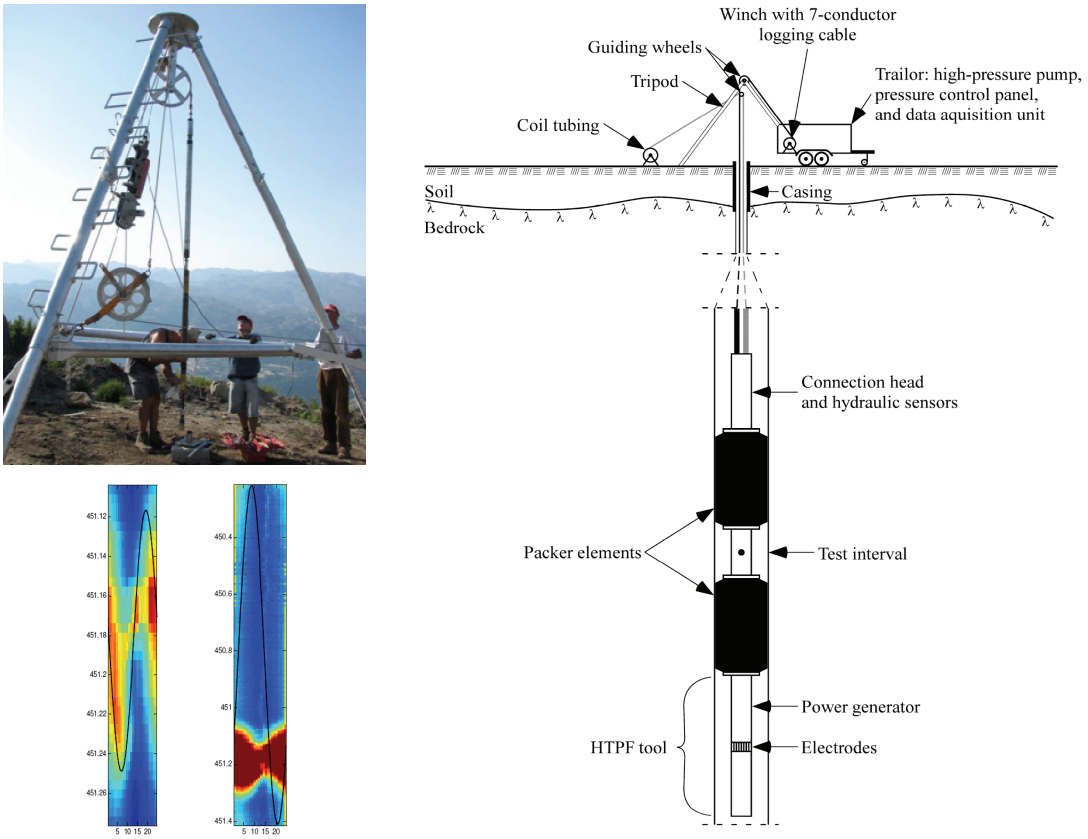


*Figure 3. Hydraulic fracturing equipment, electric image of a tested fracture and hydraulic fracturing test setup.*

## METHODOLOGY FOR GLOBAL ANALYSIS OF THE *IN SITU* STRESS FIELD

Global interpretation methodologies start by establishing a set of assumptions regarding the stress field in the rock mass. In some cases, based on the particular geometric conditions of a given problem, it may be reasonable to set forward some assumptions regarding the directions of the principal stresses. Assumptions regarding the variation of the stress components may also be justified. It is common to consider that the vertical and horizontal stresses increase linearly with depth, since the stresses are, in a large proportion, due to the weight of the overlaying ground.

The global interpretation methodology used in the analyses presented in this paper (Lamas et al., 2010) is based on the following assumptions:

- The rock mass can be modelled as an equivalent continuum, which means that any existing faults, at the scale of the excavations, do not condition the stress field significantly.

- The natural *in situ* stress is calculated for an initial situation, prior to the disturbance of the stress field caused by significant topographic or geometric changes, such as the excavation of a deep canyon by a river, or any underground excavations in the area of interest.

- The components of the initial *in situ* stresses $\sigma_j^0$ are zero at the ground surface and vary linearly with depth:

$$\sigma_j^0 = k_j \gamma h \quad \text{with } (j = 1,\ldots,6) \qquad [1]$$

where $\gamma$ is the unit weight of the rock mass and $h$ is the depth.

The existing natural stress field to be considered in design results from the initial stress field, which is characterised by the parameters $k_j$, and from the effect of the surface and underground excavations that disturbed the initial conditions. In very simple problems, the natural stress field may be calculated using analytical solutions, but in most cases, where complex geometries are involved, calculation of the natural stresses requires the use of three-dimensional numerical models of the rock mass.

Parameters $k_j$ are determined from the measured stress components obtained in all *in situ* stress measurements, which may have been carried out in distinct locations and using different methods, and from the geometry of the excavations, using the following methodology, which is derived from a procedure proposed by Sousa *et al.* (1986):

- A vector $M_i$ is assembled with the N stress components measured in the tests.

- Six loading cases, $E_j$, corresponding to the six initial stress components, $\sigma_j^0$, are applied separately in the rock mass model, using unit $k_j$ values. It is then possible to calculate the stresses $\sigma_{mj}$ (where $m$ denotes the six stress components and $j$ the six loading cases) at any point of the rock mass.

- The values of $\sigma_{mj}$ obtained for the locations where the tests were carried out can be grouped in the matrix $A_{ij}$ (where $i$ denotes the N measured stress components and $j$ the six loading cases).

- Using the principle of superposition of effects, the linear combination of the states of stress resulting from the six loading cases can be expressed by the following set of equations:

$$A_{ij}\, k_j = M_i \quad \text{with } (i = 1,\ldots,N) \text{ and } (j = 1,\ldots,6) \qquad [2]$$

This set of linear equations is usually highly redundant and can be solved by the least squares method, thus obtaining the six $k_j$ values, which characterise the most likely *in situ* stress field in the rock mass. It is then possible to calculate the natural *in situ* state of stress at any point of the rock mass, $\sigma_m$, with the following equation:

$$\sigma_m = k_j\, \sigma_{mj} \quad \text{with } (m = 1,\ldots,6) \text{ and } (j = 1,\ldots,6) \qquad [3]$$

This is a general methodology to estimate the full three-dimensional initial state of stress. However, in most instances, and in view of the limited number of test results, some additional assumptions may be considered. The most common assumptions are that the vertical initial *in situ* stress is a principal stress and its value corresponds to the weight of the overlying ground.

## GLOBAL ANALYSIS OF THE STRESS FIELD FOR THE SALAMONDE II POWERHOUSE

### Geotechnical Conditions

The Salamonde II re-powering hydroelectric scheme, promoted by EDP – Energies of Portugal S.A., includes a 2 km long underground hydraulic conduit and a powerhouse cavern. The rock mass is a good quality coarse grained granite, intersected by several fault zones (COBA, 2009). The state of stress is influenced by the complex topography of the ground. Results obtained in the stress measurement study performed to support the design were presented in detail by Espada *et al.* (2013) and are summarised in this paper.

The powerhouse cavern is 66 m long, 26.5 m wide, and 56 m high at the turbine hall, and is located on the left river bank 150 m below the ground surface. It houses one 224 MW reversible pump turbine. Figure 4(a) shows the location of the new powerhouse in relation to the original one and to the Cávado River, where the Salamonde dam is located, as well as to a tributary, the Mau River, that conditions the local topography. A three-dimensional perspective of the excavations around the powerhouse cavern is also presented in Figure 4(a). A longitudinal profile along the hydraulic conduit is shown in Figure 4(b).

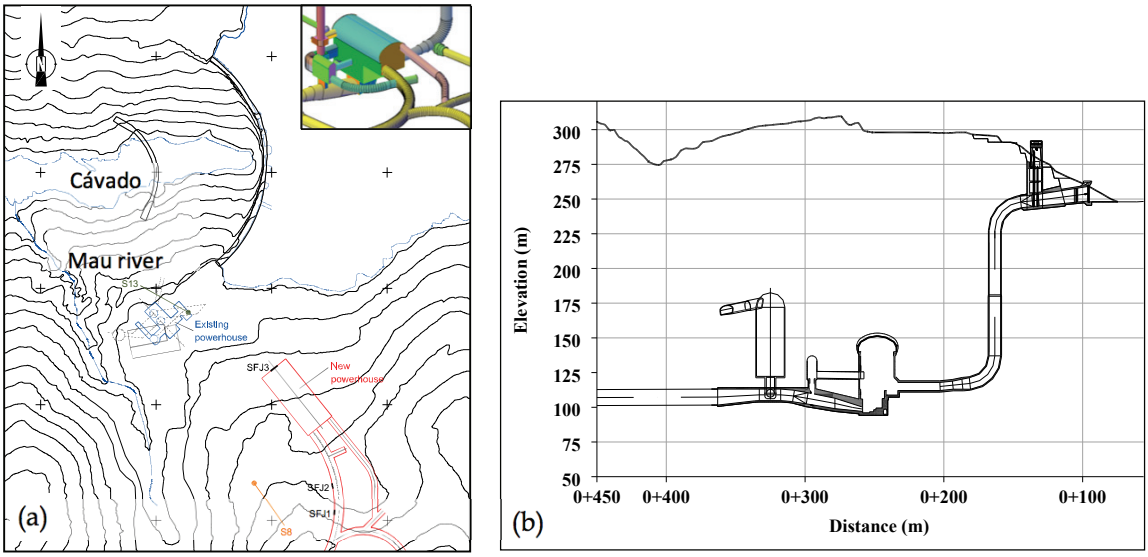


*Figure 4. Salamonde II re-powering scheme: (a) layout; (b) longitudinal profile along the hydraulic circuit*

**Stress Measurements**

Overcoring tests (STT) were performed in two boreholes (S8 and S13). Borehole S8 is vertical and starts at the ground surface, while S13 starts at the existing valve chamber, close to the original powerhouse, at a depth of 121 m, and dips at 70º (Figure 4). Three tests were carried out in each borehole, at depths between 79 m and 96 m in S8, and between 28 m and 48 m in S13. However, the results obtained in two tests in borehole S8 were doubtful, since they intersected rock joints, and they had to be discarded.

From tests conducted on the overcored rock, the values of the elastic constants needed for interpreting the test results were obtained: E = 50 GPa, ν = 0.21. In both boreholes, the maximum principal stress obtained was sub-vertical, with values around 7 MPa in S13 and around 4 MPa in S8. The sub-horizontal minimum principal stress was around 3 MPa for the three tests of S13 and 2 MPa for the test in S8.

Small flat jack tests (SFJ) were conducted in three locations identified in Figure 5(a). SFJ1 and SFJ2 were in the left wall of the powerhouse access tunnel and SFJ3 in the powerhouse North top wall, close to the roof. When the tests in SFJ3 were performed, the excavation of the powerhouse was in its initial stages, with the configuration shown in Figure 5(b), with two side drifts, three transverse galleries and three rock pillars.

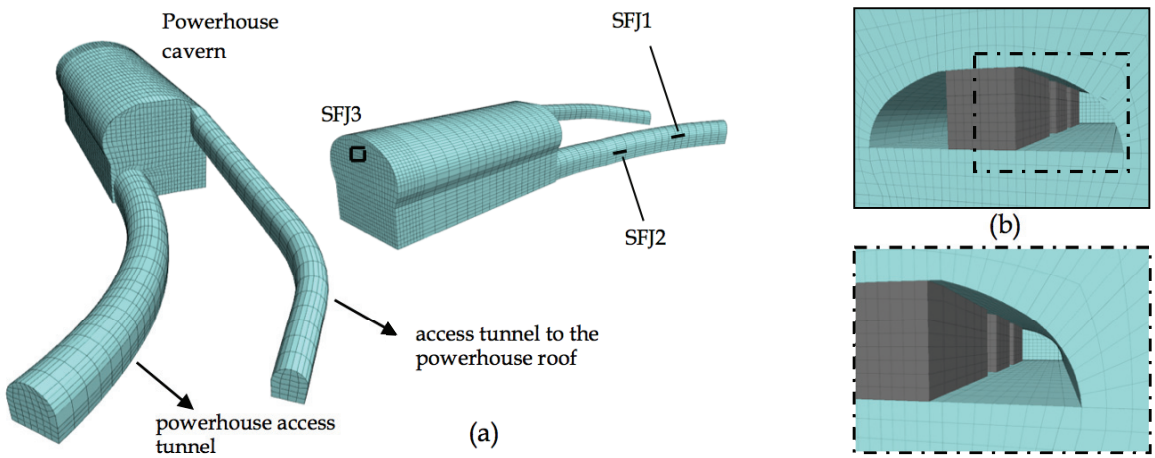


*Figure 5. Underground excavations: (a) perspective of the powerhouse and access tunnels; (b) detail of the excavation of the powerhouse roof.*

The results obtained in locations SFJ1 and SFJ2 were analysed together due to their proximity and similar lithology. The maximum and minimum principal stresses obtained are approximately 16 MPa and 6 MPa, with dip direction and dip 173º/72º and 353º/18º, respectively. In location SFJ3 the maximum and minimum principal stresses were approximately 8 MPa and 6 MPa, with dip direction and dip 225º/56º and 45º/34º, respectively.

**Three-dimensional Numerical Model**

In order to perform a global analysis of the stress state, based on the overcoring and flat jack tests results, a three-dimensional numerical model of the rock mass volume was developed with the finite difference FLAC3D program (Itasca, 2013a). The model represents the powerhouse cavern and two access tunnels (Figure 5). The topography was represented, because it is a key factor for evaluation of the stress field. Figure 6 presents a global perspective of the numerical model, a vertical section through both access tunnels and a detail of the powerhouse access tunnel.

The rock mass was assumed to be continuous, linearly elastic, homogeneous and isotropic, with an elastic modulus of 35 GPa, close to the average value obtained in the SFJ tests, and a Poisson's ratio of 0.20.

**Analysis of the *In Situ* Stress Field**

The global interpretation methodology presented earlier in this paper was used and the most likely stress field prior to the excavation was calculated. Figure 7(a) presents a vertical cross section through the middle of the powerhouse cavern with the 3D principal stress tensor (in perspective). The rotation of the obtained sub-vertical principal stress is consistent with the expected influence of the Mau River (Figure 4(a)). The major horizontal principal stress is normal to the direction of the Cávado River. Figure 7(b) presents the principal stresses in a horizontal cross section at mid-height of the powerhouse cavern.

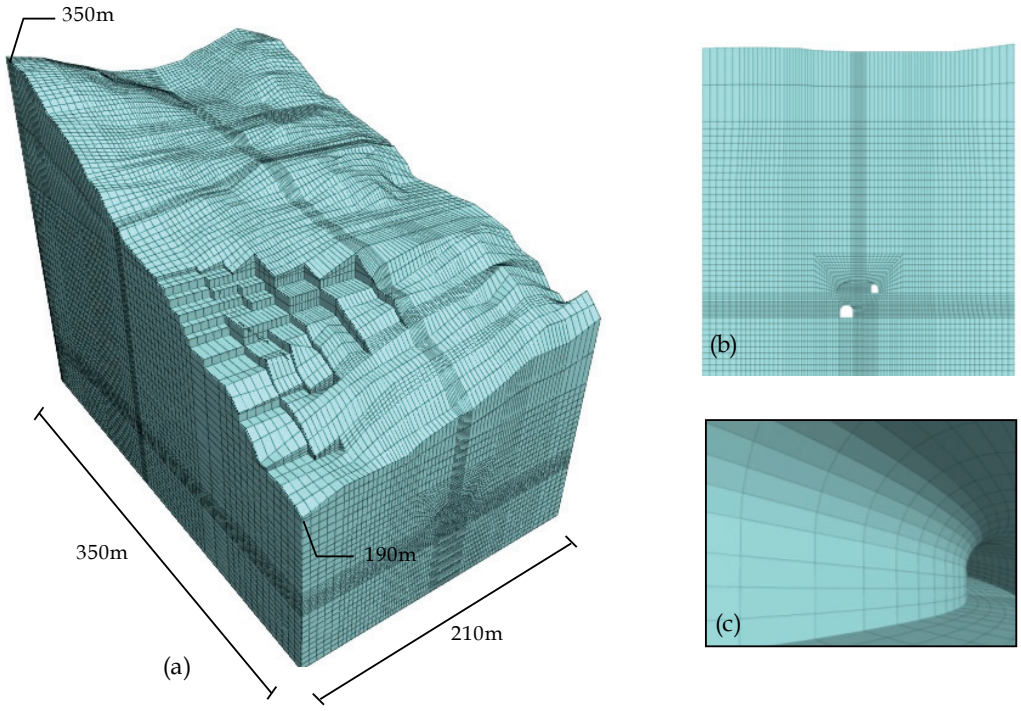


*Figure 6. Three-dimensional numerical model: (a) global perspective; (b) cross section close to the powerhouse cavern with the access tunnels; (c) detail of the powerhouse access tunnel.*

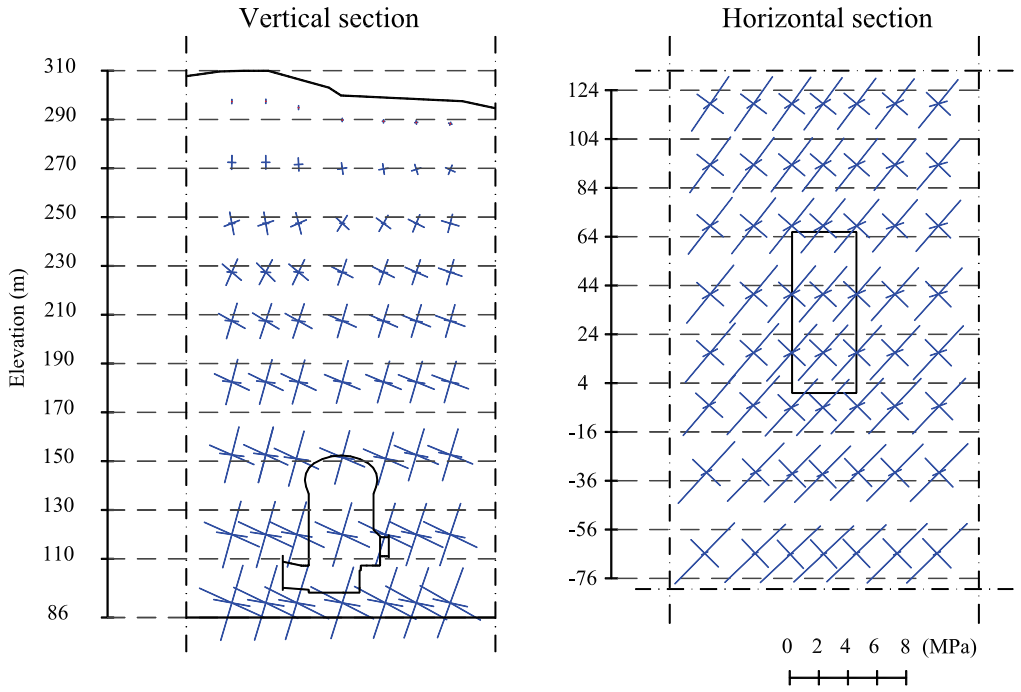


*Figure 7. Principal stresses: vertical cross section through the middle of the powerhouse cavern; horizontal cross section at mid-height of the powerhouse cavern.*

Figure 8 shows the ratio between principal stresses and vertical stress for several elevations along a vertical axis in the middle zone of the powerhouse, where the ground surface elevation is 299.9 m. After the shallow zones, the ratio of the maximum principal stress ($\sigma_I$) to the vertical stress ($\sigma_{zz}$) varies between 1.0 and 1.3, the intermediate principal stress ($\sigma_{II}$) is approximately equal to the vertical stress and the ratio of the minimum principal stress ($\sigma_{III}$) to the vertical stress varies between 0.5 and 0.6. Thus, at the powerhouse depth, $\sigma_I$ and $\sigma_{III}$ are sub-horizontal, with ratios to the vertical stress of 1.3 and 0.6 respectively, and $\sigma_{II}$ is sub-vertical.

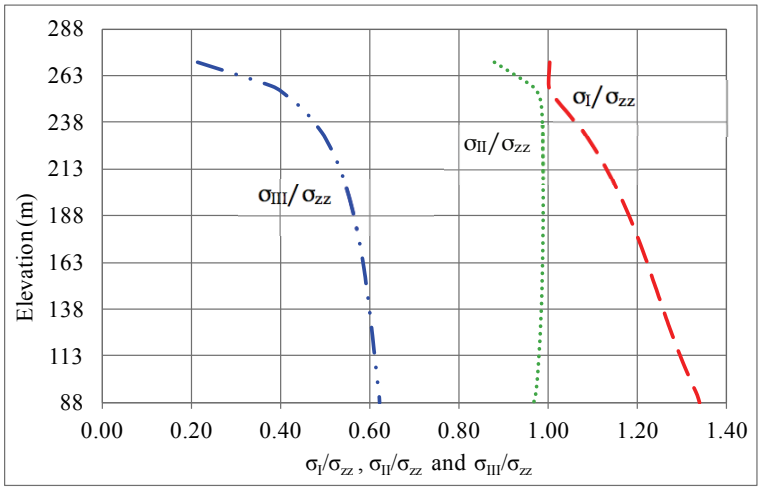


*Figure 8. Ratio between the principal stresses and the vertical stress $\sigma_{zz}$.*

## GLOBAL ANALYSIS OF THE STRESS FIELD FOR THE GOUVÃES POWERHOUSE

### Geotechnical Conditions

The Gouvães reversible hydroelectric scheme, promoted by Iberdrola, S.A., is currently in the early construction stages. The underground works comprise a 7.5 km long power conduit, two large surge chambers, and a powerhouse complex composed of a powerhouse cavern, a transformers chamber and a series of tunnels and shafts for hydraulic and access purposes. The powerhouse cavern is 20 m wide, 48 m high and 121 m long, and will be equipped with four reversible pump turbines with a total power of 880 MW.

Two different types of rock mass occur at the zone of interest to the powerhouse cavern, with a sub-horizontal contact zone (Iberdrola, 2011). The overlying rock is mica schist, with intercalations of quartz veins. Underneath the contact zone occur medium to coarse grained granites, with two micas, with intercalations of aplite and pegmatite. For the sake of simplicity, these two rock types will be called simply mica schist and granite. From the tests performed for the geotechnical characterisation before excavation of the exploration galleries started, it was concluded that the mica schist was two times more deformable than the granite.

Figure 9 is a perspective of the underground openings in the zone of the powerhouse, with the representation of the contact surface obtained by interpolation of the contact zones mapped during the excavation of the exploration galleries and obtained from borehole logs. In this paper the main aspects of the study that was conducted for estimation of the stress field are summarised (LNEC, 2016).

### Stress Measurements

In view of the different expected deformability of the two rock types, the stress measurements programme was designed assuming that significantly different stress fields could also be expected, possibly with lower horizontal stresses in the softer rock type. The tests were done when the exploratory adits were completed, and the testing programme included, in each rock type, two sets of four flat jack tests (SFJ) in perpendicular rock faces, and six overcoring tests (STT) in a vertical borehole. The combined use of these two testing methods is advantageous, because it is then possible to perform an integrated analysis of direct measurements at rock faces with indirect measurements in boreholes.

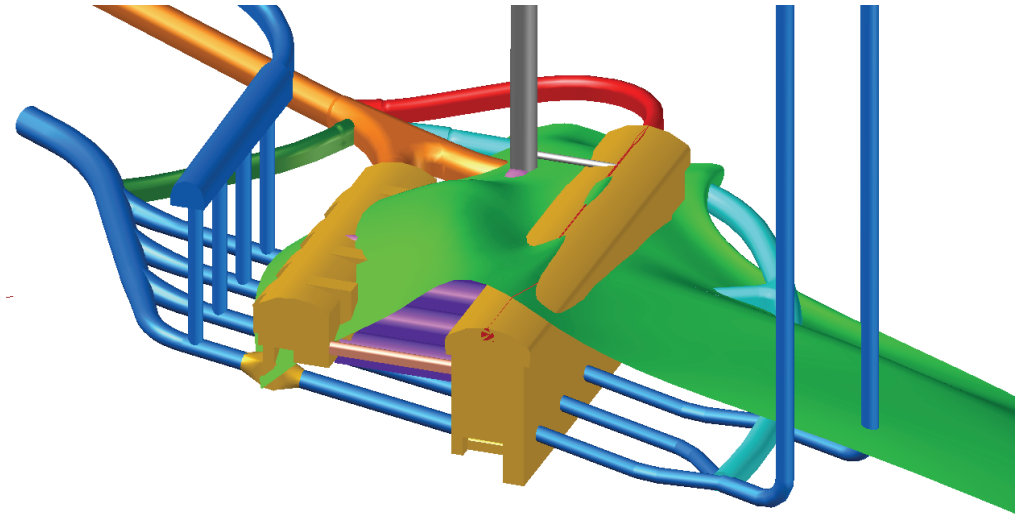

*Figure 9. Perspective of the contact surface between the mica schist (above) and the granite (underneath).*

Due to site constraints, the actual testing programme suffered some modifications, but the same principle behind the programme was kept. Figure 10 shows two perspectives with the locations of all tests and of the excavations that existed at the time they were performed.

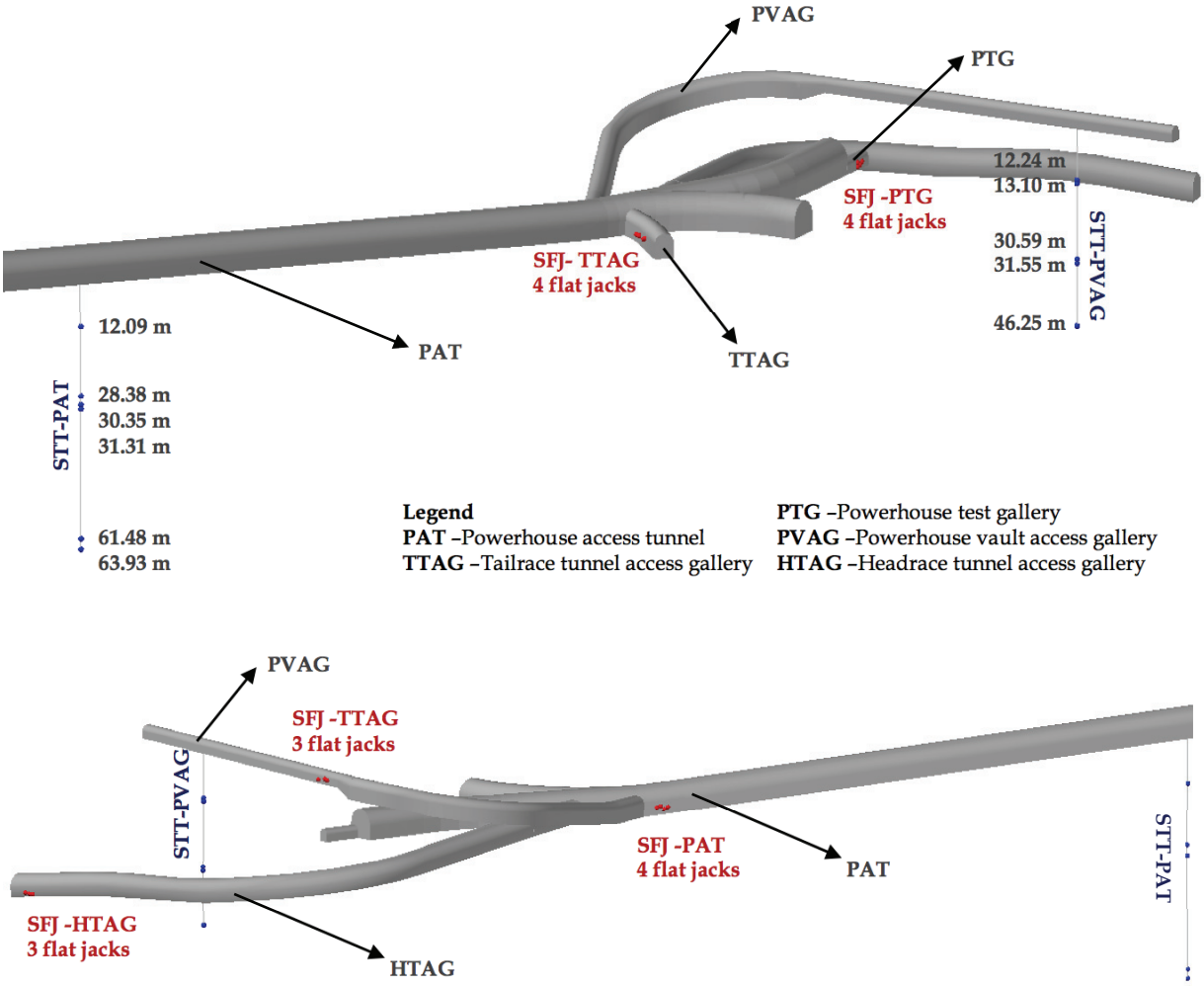


*Figure 10. Perspectives from West (above) and from East (below) of the excavations at the time of testing, showing the test locations.*

An individual analysis of the flat jack (SFJ) tests results made clear that the stress values obtained in all four tests performed in the tailrace tunnel access gallery (TTAG) were extremely low, while the elastic modulus was similar to the other tests. They were discarded, because they were found to be associated with a distressed zone in the intersection of the TTAG with the powerhouse access tunnel (PAT). A total number of 12 valid SFJ tests was obtained, six in each rock type.

Five overcoring tests were performed in granite in borehole STT-PVAG, drilled from the powerhouse vault access gallery (PVAG). However, in borehole STT-PAT, drilled from the powerhouse access tunnel (PAT), only four tests were performed in mica schist and two tests were in granite, because the contact between the mica schist and the granite was found earlier than expected. This totalled 11 valid overcoring tests, four in mica schist and seven in granite. The elastic modulus and the Poisson's ratio were measured in biaxial tests of the overcored rock specimens.

**Three-dimensional numerical model**

For the global analysis of the stress field based on the overcoring and flat jack test results, a three-dimensional numerical model of the rock mass volume was developed with the FLAC3D program. The model represents the excavations that existed at the time of the testing programme in the vicinity of the future powerhouse, as well as the ground topography. Figure 11 presents two global perspectives of the three-dimensional numerical model, showing the elevations and the location of the modelled underground excavations.

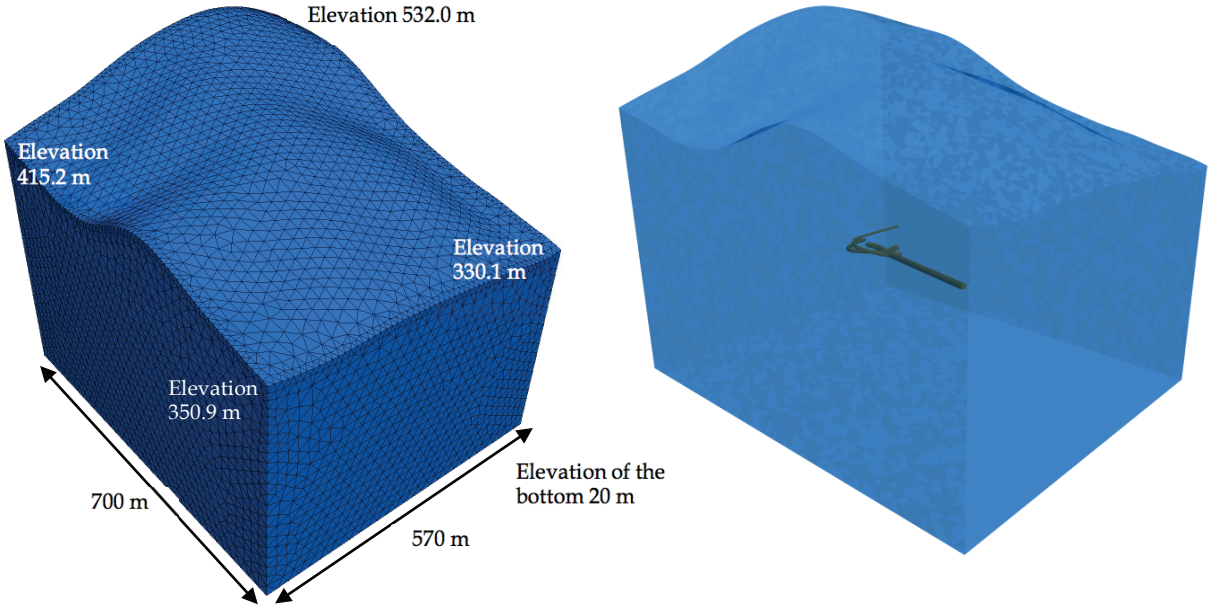


*Figure 11. Global perspectives of the three-dimensional numerical model with the location of the modelled underground excavations.*

The definition of the contact surface between the mica schist and the granite considered the information from the boreholes performed during the exploration phase and the mapping of the contact during the excavation of the access tunnels and exploration galleries represented in Figure 12. The three-dimensional model of the contact surface, obtained by interpolation, was represented in Figure 9. This surface was modelled, in a simplified way, by four planes. The numerical model, showing the contact surface and the zones of mica schist and of granite, is represented in Figure 13.

For application of the global interpretation methodology presented earlier in this paper, the vertical initial *in situ* stress was assumed to be a principal stress, resulting that four loading cases were applied separately in the numerical model. For the loading cases equivalent to initial normal stresses (one vertical and two horizontal), the boundary conditions corresponded to zero displacements normal to the lateral boundaries and zero displacements in the bottom boundary. For the loading case equivalent to initial shear stresses in the horizontal plane, the boundary conditions corresponded to zero horizontal displacements in the lateral boundaries and zero vertical displacements in the bottom boundary. Subsequently, the calculations simulated, for each loading case, the excavation of the underground works concluded until the date of the testing programme.

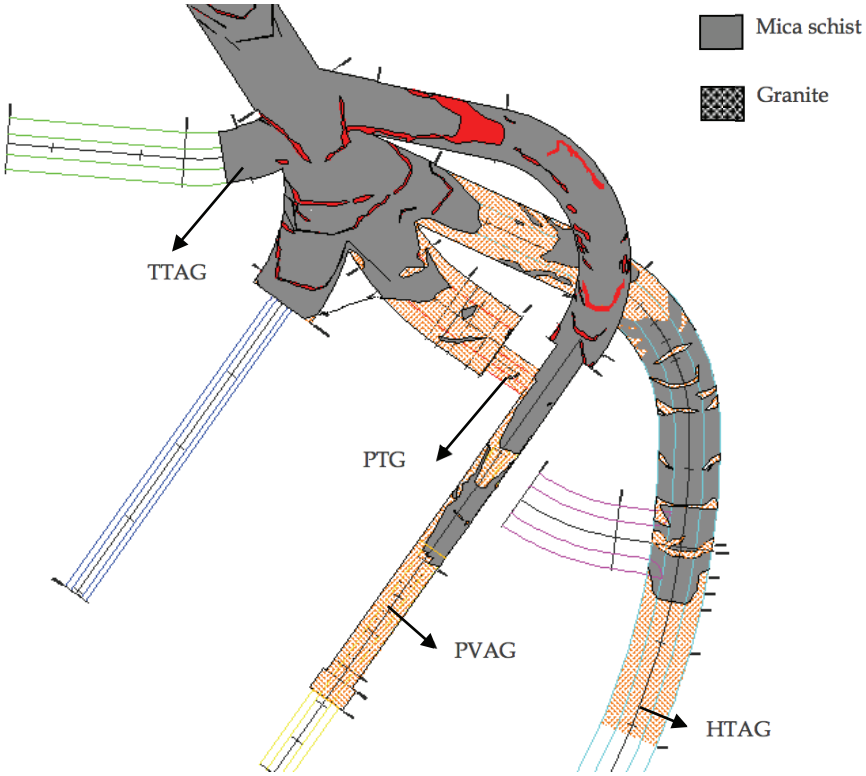


*Figure 12. Mapping of the contact between the mica schist and the granite (supplied by Iberdrola).*

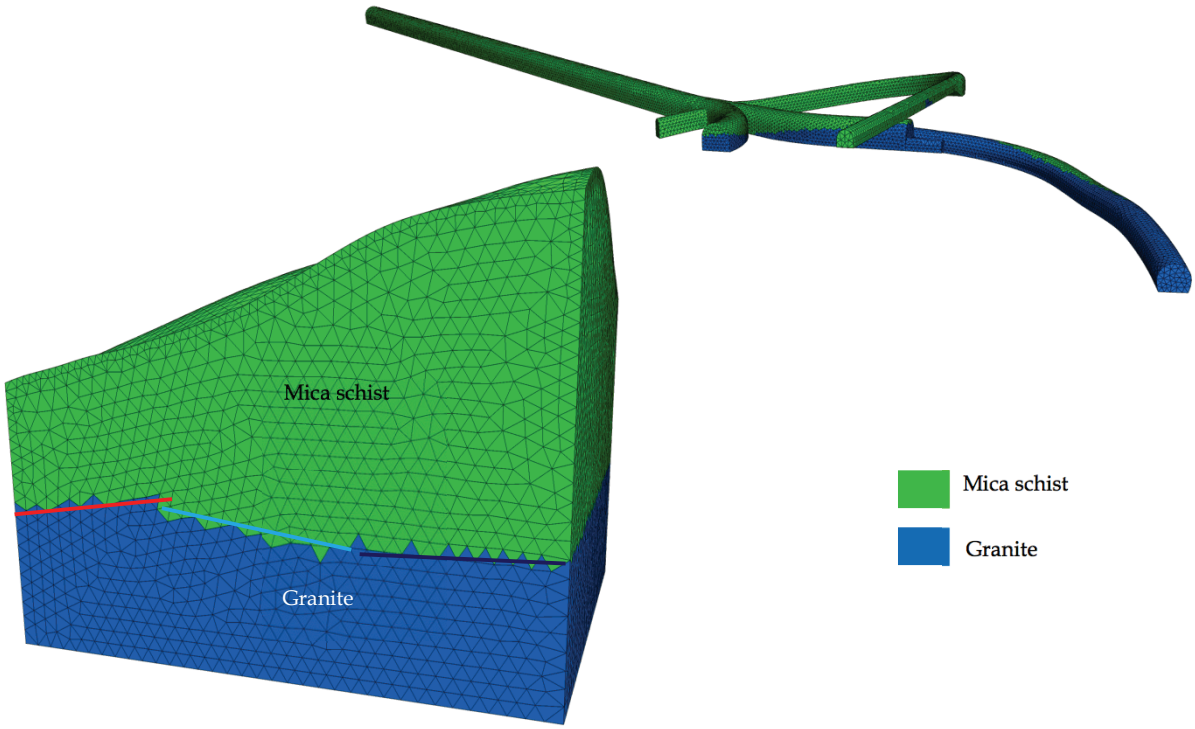


*Figure 13. Zones of the model with mica schist and granite.*

**Analysis of the *In Situ* Stress Field**

*Elastic constants*

Since two rock types occur, the values of the elastic modulus ($E$) and of the Poisson's ratio ($\nu$) are necessary for the stress field analysis. Table I presents values obtained in different ways: from lab tests in rock cores ($E_i$, $\nu$) and for the rock mass using the Hoek-Brown criterion ($E_m$) for the preliminary calculations (Itasca, 2013b); from the flat jack tests ($E_{SFJ}$); and from the recovered rock cores from the overcoring tests ($E_{STT}$, $\nu$).

*Table I. Estimated and measured elastic constants*

| Rock type | Preliminary calculations | | Hoek-Brown | Flat jack tests | Overcoring tests | |
|---|---|---|---|---|---|---|
| | $E_i$ (GPa) | $\nu$ | $E_m$ (GPa) | $E_{SFJ}$ (GPa) | $E_{STT}$ (GPa) | $\nu$ |
| Mica schist | 29.0 | 0.25 | 11.8 | 18.2 | 16.9 | 0.25 |
| Granite | 40.4 | 0.24 | 25.5 | 17.2 | 55.1 | 0.23 |

The different deformability of the intact rock for the two rock types is clear from the results in rock cores. The values obtained for $E_m$, derived from the values of $E_i$ and assumed GSI values of the rock mass, also resulted in a ratio around 2 between the elastic moduli of the granite and of the mica schist.

With regard to the only values measured on site—the $E_{SFJ}$ values—they did not confirm this difference. The measured elastic moduli of the two rock types were similar. This was in apparent contradiction with the laboratory tests, which gave much higher values for the granite rock samples. The important conclusion from the field results was that, in the case of the mica schist, the in situ behaviour of this anisotropy rock mass, at depth, with a high confinement, corresponds to a much more competent rock mass than what could be predicted from laboratory tests on rock samples. In the case of the granite, the opposite situation was encountered, because of the fracturing degree and of the intercalations of aplite and fractured pegmatite.

In view of this discrepancy, two cases were studied: a homogeneous case, where the value of the elastic modulus adopted for both rock types was 25 GPa, and a heterogeneous case, where the same value was used for the granite, but the value for the mica schist was reduced to half, *i.e.* 12.5 GPa. The Poisson's ratio was 0.24 for both rock types in both cases.

*Calculations*

In order to fully understand the effect of the rock mass heterogeneity in the results, four calculations were performed: A – a homogeneous situation, considering the results from all tests; B – a heterogeneous situation, considering the results from all tests; C – a heterogeneous situation, considering only the tests in the mica schist; D – a heterogeneous situation, considering only the tests in the granite.

Calculation A was a reference situation. The objective of calculation B was to check to which extent the close proximity between the test locations and the contact surface, where a sudden change in deformability could eventually occur, influenced the obtained stress field. Calculations C and D aimed to check if the stresses calculated in the two rock types showed important differences. The results of calculations C and D represent more accurately the stress field in the mica schist and in the granite, respectively.

In all calculations, the vertical initial *in situ* stress was assumed to be a principal stress, equal to the gravitational stress. Considering a system of coordinates where axes X and Y are normal and parallel to the powerhouse cavern axis (azimuth 125° and 35°, respectively) and the Z axis is vertical, this means that $k_{xz} = k_{yz} = 0$ and $k_{zz} = 1$.

*Results*

The values obtained for the parameters *k* in the four calculations are presented in Table II. The *k* values are representative of the rock mass stress field, with the exception of zones near the surface where the effect of topography is very important. At depth, they are approximately equal to the ratio between the stress and the gravitational vertical stress. The *k* values can, therefore, be directly used for the analysis of the rock mass stress field prior to the excavation.

*Table II – Results obtained for the parameters k*

| *k* | Homogeneous situation | Heterogeneous situations | | |
|---|---|---|---|---|
| | A - Mica schist + Granite | B – Mica schist + Granite | C – Mica schist | D - Granite |
| $k_{xx}$ | 0.68 | 0.70 | 0.58 | 0.77 |
| $k_{yy}$ | 1.21 | 1.20 | 1.22 | 1.18 |
| $k_{xy}$ | 0.10 | 0.10 | 0.16 | 0.05 |

The *k* values for calculations A and B are very similar, and this confirms that the tests were adequately located at a sufficient distance from the contact surface, so that the test results were not affected by the close proximity to a zone with contrasting deformabilities. The horizontal stresses normal to the powerhouse axis are 30% lower than the vertical stresses, and parallel to the powerhouse axis are 20% higher. The shear stresses are 10% of the vertical stresses. The difference between the horizontal stresses is higher for calculation C and lower for calculation D.

The *k* parameters and the azimuth that correspond to the principal stresses and directions were also calculated and are presented in Table III. For calculations A and B, the maximum and minimum horizontal stresses are 1.23% and 67% the vertical stresses. For calculation C, only with the tests on mica schist, there is a large difference between the maximum and minimum principal horizontal stresses, of 126% and 54%, respectively. For calculation D, only with the tests on granite, the corresponding values are 119% and 77% respectively. The principal directions only vary slightly in the different calculations.

*Table III – Results obtained for the principal stresses and directions*

| Principal stress | Homogeneous situation | | Heterogeneous situations | | | | | |
|---|---|---|---|---|---|---|---|---|
| | A - Mica schist + Granite | | B - Mica schist + Granite | | C - Mica schist | | D - Granite | |
| | *k* | Azimuth | *k* | Azimuth | *k* | Azimuth | *k* | Azimuth |
| V | 1.00 | vertical | 1.00 | vertical | 1.00 | vertical | 1.00 | vertical |
| $H_{max}$ | 1.23 | 45º | 1.22 | 46º | 1.26 | 49º | 1.19 | 42º |
| $H_{min}$ | 0.66 | 135º | 0.68 | 136º | 0.54 | 139º | 0.77 | 132º |

All calculations were repeated without assuming $k_{zz} = 1$. There was only a slight decrease of 10% to 15% in the calculated vertical stresses. The value and the direction of the principal horizontal stresses were very similar to the previous calculations. This was considered as a good calibration of the test results and of the methodology of analysis, as well as a validation of the assumptions.

*Analysis of the results*

The global interpretation methodology presented earlier in this paper was used and the most likely stress field prior to the excavation was calculated. Figure 14 represents the principal stresses for calculation B in a horizontal plane and a vertical plane, where the excavations are represented only for reference.

Figure 15 is a representation of the principal stresses and directions at two points close to the contact surface, one in mica schist (elevation 233.0 m), and the other one in granite (elevation 170.6 m), obtained

for calculation B (with all tests) and for calculations C (with the tests in mica schist) and D (with the tests in granite). The principal directions are similar in both cases. The directions of the maximum and minimum principal stresses are sub-horizontal. The maximum principal stress is approximately parallel to the river Tâmega valley and to the powerhouse cavern axis.

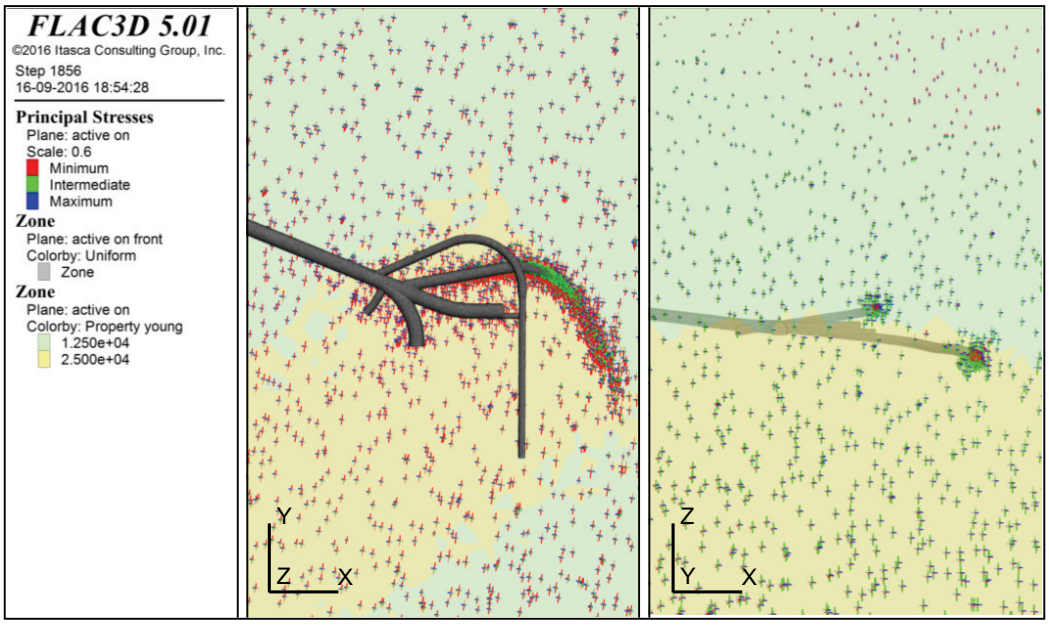


*Figure 14. Initial principal stresses for calculation B (mica schist in green, granite in yellow): (a) in a horizontal plane at mid height of the powerhouse cavern; (b) in a vertical plane normal to the powerhouse cavern axis.*

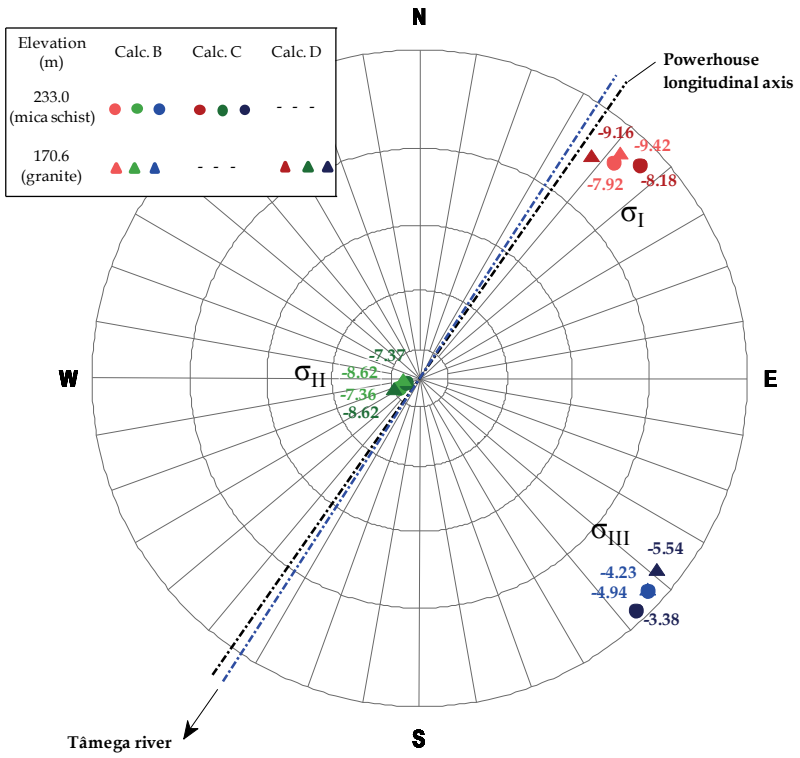


*Figure 15. Lower hemisphere stereographic projection with the principal directions and stresses (in MPa) for calculations B, C and D.*

Figure 16 presents the principal stress profiles with depth for calculation B, together with the stress profiles in the mica schist for calculation C and in the granite for calculation D. The stress ratios vary with depth, mainly near the surface, and are little influenced by the topography at the powerhouse cavern depth. It is interesting to observe the difference between the profiles obtained for calculation B and for calculations C and D. In the latter, there is a pronounced increase of the minimum principal stress from the mica schist to the granite, and an opposite effect, but not so pronounced, is observed for the maximum principal stress.

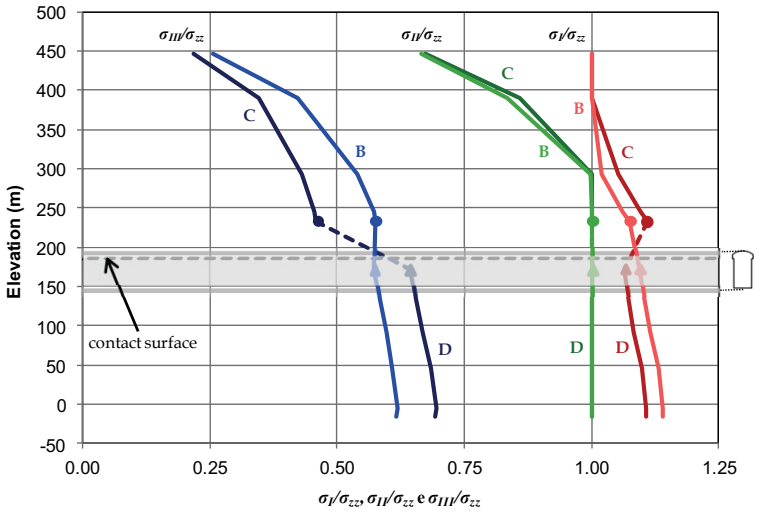


*Figure 16. Ratio between the principal stresses and the vertical stress for calculations B, C and D (the markers represent the points in Figure 15).*

## TIME DEPENDENT EFFECTS AT PARADELA II SITE

### Paradela II

The planned Paradela II reversible hydroelectric scheme, on the Cávado River, promoted by Energies of Portugal – EDP, has a 10 km long power conduit, with a powerhouse located halfway in the conduit, at the depth of 500 m, in a good quality granite rock mass (Figure 17). The powerhouse will be equipped with one 318 MW reversible pump turbine.

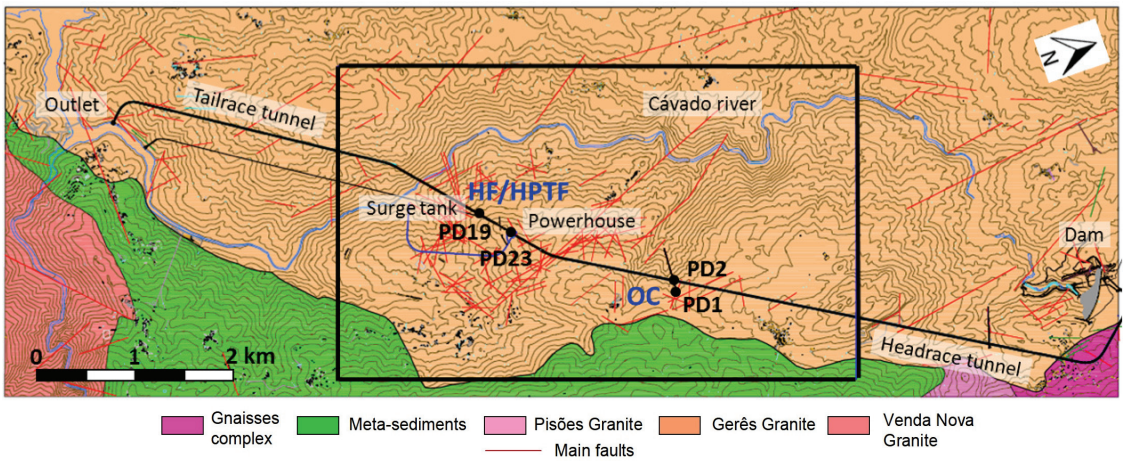


*Figure 17. Layout of the Paradela II scheme with the location of the overcoring (OC) and hydraulic (HF/HTPF) stress measurements.*

For determination of the stress field down at the depth of the powerhouse, the University of Strasbourg, with LNEC's support, carried out HF and HPTF tests in two 500 m deep boreholes (PD19 and PD23). Stress measurements were carried out by overcoring in two vertical boreholes (PD1 and PD2), drilled from an existing adit, at test depths from 160 m to 250 m. The test locations are indicated in Figure 17.

Exploration of the results of all the tests performed at this site resulted in a doctoral thesis (Figueiredo, 2013) (Figueiredo *et al.*, 2014). A very large FLAC3D model was used for the interpretation of the *in situ* tests results. The model included the topography of this mountainous region and the locations where the tests were carried out. The detailed elevations of the simulated area and the numerical model mesh are shown in Figure 18. The maximum difference in elevation is about 715 m. The model is 5 km long, 3 km wide and 2.5 km deep.

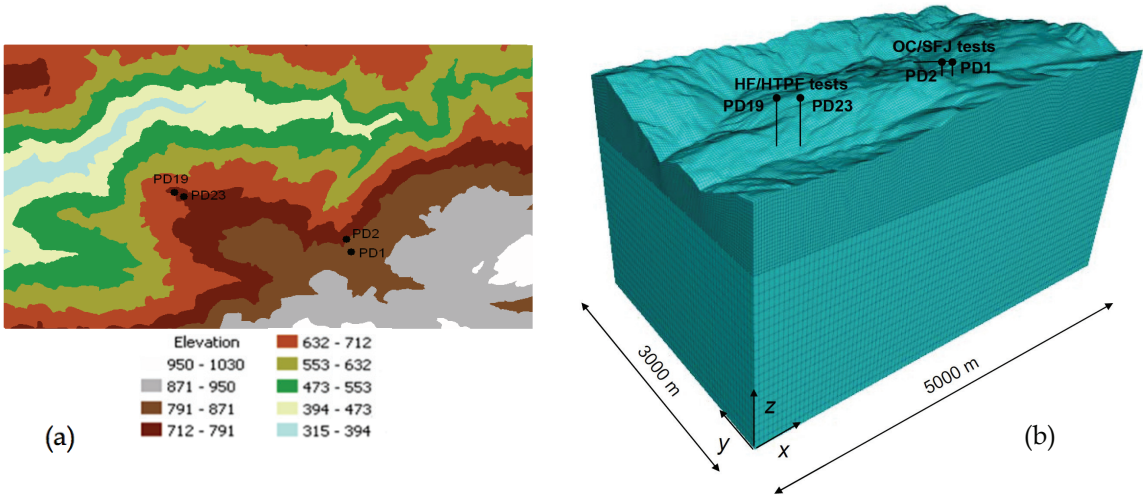


*Figure 18. Paradela II: (a) detailed elevation considered; (b) global perspective of the numerical model.*

One of the objectives of this study was to investigate how gravitational stresses compare with the measured stress values. A discrepancy was found between the calculated and the measured horizontal stresses: they are much higher *in situ* than those predicted by the model. Several possible explanations, such as tectonic forces, rock mass heterogeneities, large discontinuities, faults and time dependent effects, were investigated.

Time dependent effects were found to justify the measured horizontal stresses. The reason for this is that, whereas the elastic behaviour considered in the model can be adequate to reproduce mechanical processes occurring in rock masses over short periods of time, it cannot tackle the modelling of geological phenomena involving very long time scales, because, even at low temperatures, rocks exhibit time dependent behaviours, such as creep and relaxation.

In a homogeneous medium with linear elastic behaviour, such as the rock mass considered in the numerical model, time dependent effects can be simulated by a Maxwell viscoelastic model by increasing the Poisson's ratio and decreasing the elastic modulus (Amadei and Stephansson, 1997). Ultimately, a Poisson's ratio of 0.5 would result in hydrostatic stresses, which is the limit to which Maxwell's viscoelastic model tends for infinite time. The elastic modulus would tend to zero, but in stress analysis such as this one, its value is irrelevant. In this case, the "equivalent" Poisson's ratio that rendered the best approximation between the measured and calculated horizontal stresses was 0.47.

Figure 19 presents the variation with depth of the normal stresses measured in the fractures where hydraulic tests were performed and the corresponding calculated values with the viscoelastic model. In this figure, a 99% confidence interval for the measured normal stresses is presented. This analysis shows that for eleven of the fifteen tests the difference between the measured and calculated values is smaller than 1.0 MPa, and that the remaining tests have discrepancies between 1.2 and 1.3 MPa.

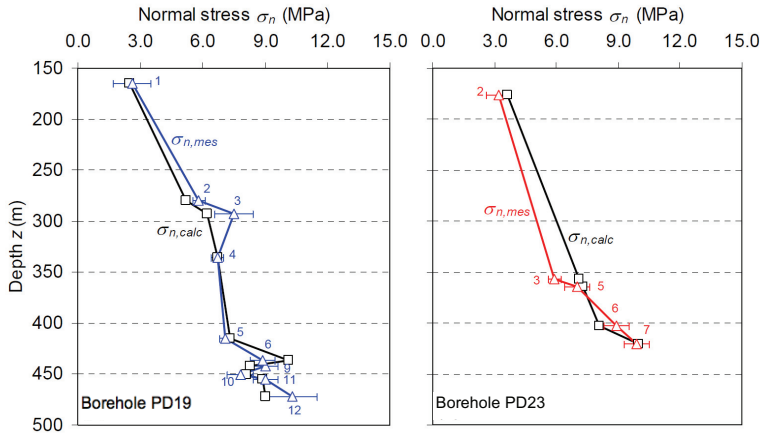


*Figure 19. Normal stresses measured in hydraulic tests ($\sigma_{n,mes}$) and calculated with a viscoelastic model ($\sigma_{n,calc}$).*

An inversion analysis of all hydraulic tests results shown in the previous figure was carried out. An interval of 99% confidence was considered for the stress profiles that resulted from the inversion. The resulting principal stress profiles, where $\sigma_I$ is vertical, are displayed in Figure 20. It shows a good agreement with the values calculated by the viscoelastic model.

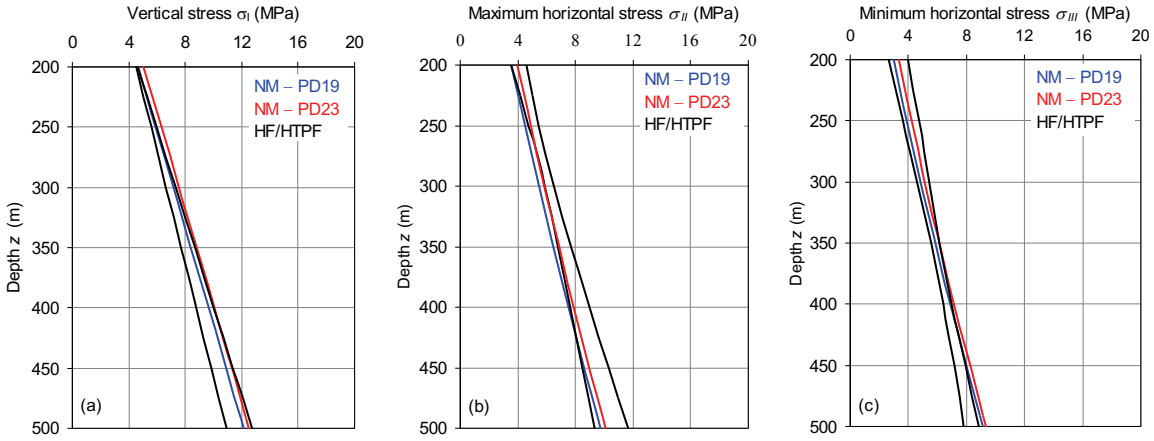


*Figure 20. Stress profiles obtained from the hydraulic test results (HF/HTPF) and the viscoelastic model (NM).*

Vertical profiles of the principal stresses were determined using the viscoelastic model at the locations where the overcoring tests were performed in order to compare their results. The values obtained are presented in Figure 21.

Except for the sub-vertical stress ($\sigma_I$) in one of the boreholes, which is often over-estimated by overcoring tests, and of the stresses obtained close to the existing adit, the agreement between measured and calculated sub-horizontal principal stresses is generally satisfactory, with differences smaller than 1.5 MPa. At the midpoint of the measurements provided by the overcoring tests, the discrepancy between results from hydraulic and overcoring tests is smaller than 1.0 MPa. This is so despite the distance of about 1.5 km between both test locations.

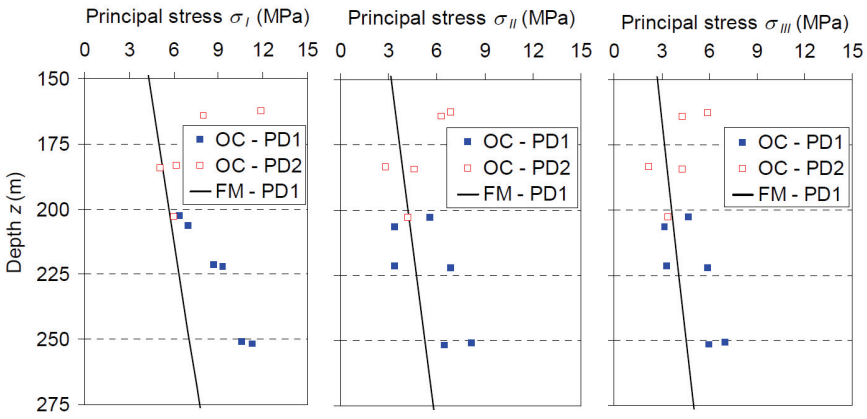


*Figure 21. Stresses obtained from the overcoring test results (OC) and the viscoelastic model (FM).*

## TIME DEPENDENT EFFECTS AT SALAMONDE II SITE

### Salamonde II

The same type of analysis presented for Paradela II, considering time dependent effects, was also reproduced for the Salamonde II site. The objective of this study was to investigate to what extent could time dependent effects influence the horizontal stresses calculated in the global stress analysis presented above, which are higher than those obtained in a gravitational analysis with the "short term" value of the Poisson's ratio of 0.20 that was used. New calculations were carried out with the three-dimensional numerical model of Salamonde II. They were gravitational analyses, but with increasing values of the Poisson's ratio, until the resulting minimum horizontal stress reached a best fit, which is approximately 0.6 times the vertical stress at the depth of the powerhouse. The "long term" Poisson's ratio obtained by this process was 0.40.

Figure 22 presents the principal stresses obtained in a horizontal section through the middle of the powerhouse cavern for the two types of analysis performed. On the left-hand side are the results obtained with the inverse analysis of the test results presented above. On the right-hand side are the results of a simple gravitational analysis with a Poisson's ratio of 0.40. In this latter analysis, a nearly hydrostatic horizontal stress field was calculated, and therefore the stress orientations are not very well defined.

Figure 23 shows the ratio between the principal stresses and the vertical stress for the gravitational, time dependent analysis with a Poisson's ratio of 0.40. Comparison of Figures 8 and 23 suggests that the *in situ* stress state is influenced by the topography and has components due to gravity and time dependent effects, superimposed with stresses of other origins, such as tectonic forces, or resulting from the localized effect of important discontinuities or heterogeneities.

## CONCLUSIONS

The aim of all the studies presented in this paper was to obtain meaningful estimates of the stress field to be used in the design of underground structures such as powerhouse caverns. For this purpose, an inverse methodology was used. It integrates the results of *in situ* stress measurements obtained by various methods, so that the most likely stress field in the zone of interest for the design of the underground structures is obtained. For applying this methodology to the Salamonde II and Gouvães powerhouses, large three-dimensional numerical models of the rock mass representing the ground topography, the lithology and the underground openings had to be developed. The results obtained were presented and analysed.

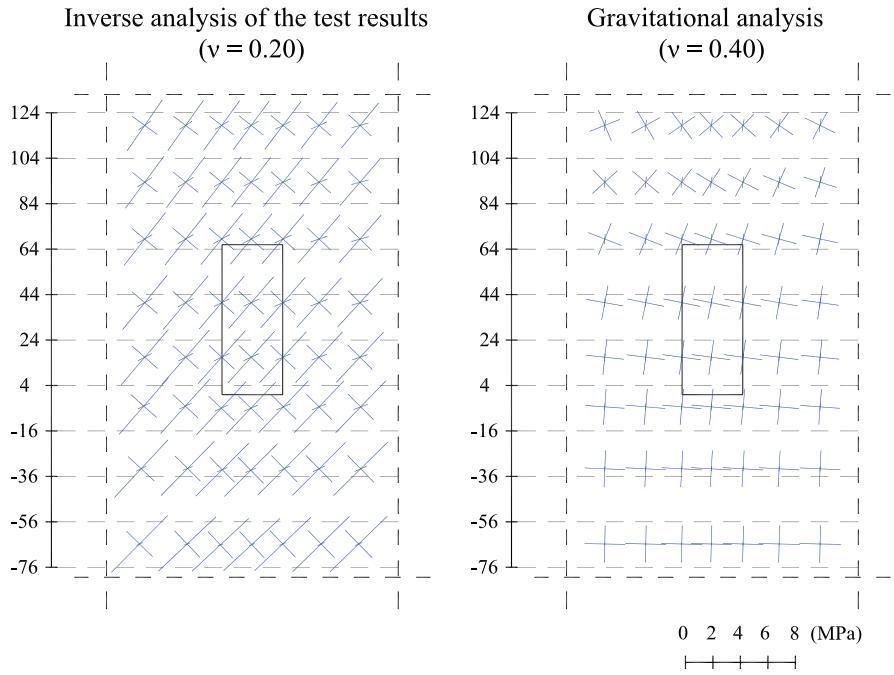


*Figure 22. Principal stresses in a horizontal section through the middle of the powerhouse cavern.*

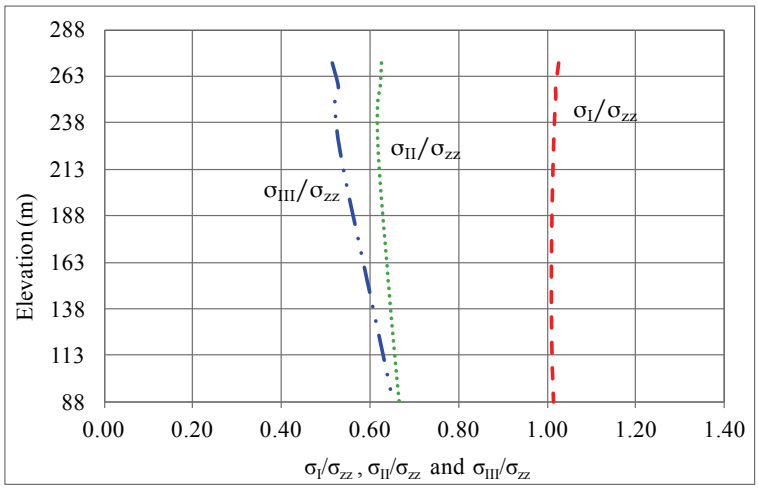


*Figure 23. Ratio between the principal stresses and the vertical stress for a gravitational analysis with a Poisson's ratio of 0.40.*

Studies of the *in situ* stress field for a specific site should be developed in an integrated way, from the early stages of definition of the stress measurement programme. Tests should be conducted in locations allowing to capture key features of the stress field variation and should also have in mind the numerical model that will be used for the analysis of the results and the global interpretation model deemed adequate for each project.

Sometimes, boreholes can reach the rock mass around an underground structure enabling overcoring and hydraulic fracturing tests to be performed, but in other cases depth may make them unfeasible. These difficulties may be overcome by performing additional tests as soon as exploratory or access adits reach the underground structures zone, namely using direct measurements such as flat jack tests, and in this way, update the values of the stress field.

The number of *in situ* stress measurements to support the design is often limited. This was also the case of the examples presented. Therefore, it is usually impossible to make any statistical inference about stress variability. Thus, the obtained most likely *in situ* stress field should be used as a reference situation for design, and judicious sensitivity analyses should also be performed.

The two different rock types existing at the Gouvães site and the location of the contact surface, which intersects the powerhouse cavern, made it necessary to adopt a special strategy to locate the stress measurements and to model this heterogeneous medium. Consideration of the different deformability of the two rock types was found essential to reach correct stress field estimates.

Finally, results of studies carried out to investigate the influence of time on the observed large-scale stress field, at a geological time scale, were presented. Calculations considering time dependent effects were presented for the Paradela II and Salamonde II sites, by applying in the numerical model relaxed elastic properties to simulate a viscoelastic behaviour. The results demonstrate that *in situ* stresses are influenced by topography and have a component due to gravity and time dependent effects, superimposed with stresses resulting from the regional or local influence of important discontinuities or heterogeneities, or with stresses from other origins such as tectonic forces.

## ACKNOWLEDGEMENTS

Permission from EDP - Energies of Portugal, S.A. to publish information regarding the studies for the Paradela II site and Salamonde II hydroelectric scheme, and from Iberdrola S.A. to publish information regarding the studies for the Gouvães powerhouse is greatly acknowledged.

## REFERENCES

Amadei, B. and, Stephansson, O. (1997). *Rock Stress and its measurement*. Chapman & Hall.

COBA (2009). Design of the re-powering of the Salamonde hydroelectric scheme. Lisbon.

Cornet, F.H. (1993). Stress in rock and rock masses. *Comprehensive Rock Engineering*, Volume 3. Hudson, J. (ed.). Pergamon Press, Oxford, pp. 297-327.

Espada, M.; Lamas, L.; Leitão, N. and Figueiredo, B. (2013). Global methodology for evaluation of the stress field in a rock mass from in situ tests. Application to the Salamonde II powerhouse cavern. *Proceedings of EUROCK 2013 – Rock Mechanics for Resources, Energy and Environment*. Kwasniewski, M. and Lydzba, D. (eds). Taylor & Francis, pp. 425-430.

Figueiredo, B. (2013). Integration of in situ stress measurements in a non-elastic rock mass. PhD thesis, University of Strasbourg, France.

Fairhurst, C. (2003). Stress estimation in rock: a brief history and review. *International Journal of Rock Mechanics and Mining Sciences*, Volume 40, pp. 957-973.

Figueiredo, B.; Cornet, F.H.; Lamas, L. and Muralha J. (2014). Determination of the stress field in a mountainous granite rock mass. *International Journal of Rock Mechanics and Mining Sciences*, Volume 72, pp. 37-48.

Hudson, J.A.; Cornet, F.H. and Christiansson, R. (2003). ISRM Suggested methods for rock stress estimation – Part 1: Strategy for rock stress estimation. *International Journal of Rock Mechanics and Mining Sciences*, Volume 40, pp. 991-998.

Iberdrola (2011). Gouvães hydroelectric scheme, General memoire, Annex 2, Geological and Geotechnical study, Volume 1 (in Portuguese).

Itasca (2013a). FLAC3D - Fast Lagrangian Analysis of Continua in 3 Dimensions, Version 5.01, User's Manual. Itasca Consulting Group, Minneapolis, USA.

Itasca (2013b). Numerical modelling of the construction process of the Gouvães cavern for the new design conditions (in Spanish). Itasca Consultores S.L., Astúrias, Spain.

Laigle, F. and Plassart, R. (2015). Design methodology for large underground powerplants. *Proceedings of the 13th ISRM International Congress on Rock Mechanics*. Montréal, Canada. CIM and ISRM.

Lamas, L.; Muralha, J. and Figueiredo, B. (2010). Application of a global interpretation model for assessment of the stress field for engineering purposes. *Rock Stress and Earthquakes.* Xie, F. (ed.). *Proceedings of the 5th International Symposium on In-Situ Rock Stress*. Taylor & Francis, pp: 631-636.

Ljunggren, C.; Chang, Y.; Janson, T. and Christianson, R. (2003). An overview of rock stress measurement methods. *International Journal of Rock Mechanics and Mining Sciences*, Volume 40, pp. 975-989.

LNEC (2016). Underground Works of the Gouvães Powerhouse. Determination of the Initial State of Stress (in Portuguese). LNEC report 277/2016 – DBB/NMMR. Lisbon, Portugal. 97 pp.

Sousa, L.R.; Martins, C.S. and Lamas, L.N. (1986). Development of the techniques of measurement and interpretation of the state of stress in rock masses. *Proceedings of the IAEG International Congress*, Buenos Aires.

## Luís Lamas

Senior Research Officer (at LNEC), Secretary General (at ISRM)
LNEC – Portuguese National Laboratory for Civil Engineering
and ISRM – International Society for Rock Mechanics

Luís Lamas graduated in Civil Engineering from the University of Lisbon, and obtained a MSc and a PhD in Rock Mechanics at the Imperial College of Science and Technology in London.

He is currently a Senior Researcher and Head of the Modelling and Rock Mechanics Unit at the Portuguese National Laboratory for Civil Engineering – LNEC and Secretary General of the International Society for Rock Mechanics - ISRM.